Identification of reduced and uncoupled models in vibroacoustical experimental modal analysis

Sifeng Bi[1], Marianne Sagnard[1], Emmanuel Foltête[1], Morvan Ouisse[1], Arnaud Jund[2]
[1]Femto-ST Institute, Department of Applied Mechanics, University of Bourgogne Franche-Comté
25000 Besancon, France
e-mail: **morvan.ouisse@femto-st.fr**

[2]PSA Groupe, Research and Development Division, Centre technique de Belchamp
25218 Montbéliard Cedex, France

Abstract

To control the noise level of passenger compartment is one of the important design issues in fields such as automobile and manned aerospace. An uncoupled model of the acoustic part extracted from the coupled vibroacoustical system is significant for predicting and improving the vehicle noise performance. The objective of this work is to build mass, stiffness, and damping matrices of a reduced equivalent system which exhibits the same behavior as the full size one. An extension of the least-square complex frequency-domain (LSCF) method is introduced specifically for vibroacoustical identification. The QR decomposition is subsequently performed to obtain a reduced model whose behavior is as close as possible to the measurement. The properness condition enforcement method employed here provides the optimal eigenvectors, which can be safely used to reconstruct the equivalent system. A simulated case study is proposed to illustrate the application of this approach.

1 Introduction

Identification of analytical models from measurements remains an important issue in experimental modal analysis. The specific vibroacoustical application pushes model identification into a more challenging battle, where not only the global coupled system but also the uncoupled structural/acoustic part of the system should be identified [1, 2]. The behavior of the uncoupled acoustic part is significant for designers to control the noise level of passenger compartment in fields such as automobile and manned aerospace. For cases with large number of sensors in the experiment, the number of degrees of freedom (dofs) of the model may be too large, leading to a huge calculation burden for their further application. In this case, being able to identify the models with a smaller size, i.e. with reduced dofs, is another common and important aspect in model identification [3, 4].

The objective of this work is to identify a reduced and uncoupled model which can represent the same behaviors as the experimentally measured ones. One of the ways to construct the system matrices is to start from the identified complex modes. The reconstruct procedure from the modes to the matrices, i.e. the inverse procedure, is quite sensitive to the noise coming from the experiment and reduction procedures, leading to a large change in the final represented system behaviors compared with the original ones. To deal with this difficulty, this work focus on a specific point named as the properness condition, described with various names in different literatures [5-7]. This condition is automatically fulfilled by the exact complex modes of the system without noise. Under this sense, the directly identified complex modes should be optimized to make sure the properness condition is enforced, so that the complex modes can be safely used in the inverse procedure to reconstruct the system matrices.

This paper proposes an integrated process including identification, reduction, and optimization techniques, after which a reduced and uncoupled model of the original vibroacoustical system is obtained. The specific topology of vibroacoustical problem is described and the corresponding non-symmetric second-order formulation is analyzed by state-space representation. As a specific non-symmetric case, the right and left complex modes are identified by an extended LSCF technique. The QR decomposition is subsequently performed on the complex modes to reduce the size of the original models. The so-called “over-properness” enforcement method [8] is specially designed for this vibroacoustical application, which is employed herein to optimize the complex modes before reconstructing the system matrices. A large size simulated case study is presented to illustrate and evaluate each of the techniques proposed in the approach.

2 The eigenvalue problem of vibroacoustical systems

2.1 Description of the vibroacoustical system

The typical structural dynamic problem is represented as

$$\mathbf{M}\ddot{\mathbf{q}}(t)+\mathbf{C}\dot{\mathbf{q}}(t)+\mathbf{K}\mathbf{q}(t)=\mathbf{f}(t) \tag{1}$$

where $\mathbf{q}(t)$ is the vector of the system response; $\mathbf{f}(t)$ is the excitation vector; $\mathbf{M}$, $\mathbf{C}$, and $\mathbf{K}$ are respectively the mass, damping, and stiffness matrices, which are typically symmetric.

The vibroacoustical system can be typically represented as the fluid domain (i.e. cavity) surrounded by the elastic structure. Response of this system is described based on natural fields which are directly measured from different parts, i.e. displacement of the structure and acoustic pressure of the cavity. Then the system has a specific topology as

$$\begin{bmatrix}\mathbf{M}_s & \mathbf{0}\\ \mathbf{L}^T & \mathbf{M}_a\end{bmatrix}\begin{Bmatrix}\ddot{\mathbf{x}}(t)\\ \ddot{\mathbf{p}}(t)\end{Bmatrix}+\begin{bmatrix}\mathbf{C}_s & \mathbf{0}\\ \mathbf{0} & \mathbf{C}_a\end{bmatrix}\begin{Bmatrix}\dot{\mathbf{x}}(t)\\ \dot{\mathbf{p}}(t)\end{Bmatrix}+\begin{bmatrix}\mathbf{K}_s & -\mathbf{L}\\ \mathbf{0} & \mathbf{K}_a\end{bmatrix}\begin{Bmatrix}\mathbf{x}(t)\\ \mathbf{p}(t)\end{Bmatrix}=\begin{Bmatrix}\mathbf{F}_s(t)\\ \dot{\mathbf{Q}}_a(t)\end{Bmatrix} \tag{2}$$

where $\mathbf{x}(t)$ is the vector of displacement of the structure, $\mathbf{p}(t)$ is the vector of acoustic pressure of the cavity, $\mathbf{F}_s(t)$ is the vector of the excitation on the structure, $\dot{\mathbf{Q}}_a(t)$ is the acoustic excitation source (volume acceleration) in the cavity. $\mathbf{M}_s$ and $\mathbf{K}_s$ are respectively the mass and stiffness matrices of the structure; $\mathbf{M}_a$ and $\mathbf{K}_a$ are respectively the mass and stiffness matrices of the cavity; $\mathbf{C}_s$ and $\mathbf{C}_a$ are respectively the structural and acoustic losses; $\mathbf{L}$ is the coupling matrix.

It is obvious that the system matrices of vibroacoustical problem are no longer symmetric. For this non-symmetric system, the right and left modes are required to solve the associated quadratic eigenvalue problem [7]:

$$(\mathbf{M}\lambda_i^2+\mathbf{C}\lambda_i+\mathbf{K})\boldsymbol{\varphi}_{Ri}=0\,, \tag{3}$$

and

$$(\mathbf{M}^T\lambda_i^2+\mathbf{C}^T\lambda_i+\mathbf{K}^T)\boldsymbol{\varphi}_{Li}=0\,, \tag{4}$$

where λ_i is the i-th eigenvalue associated to the i-th right eigenvector $\boldsymbol{\varphi}_{Ri}$ and the i-th left eigenvector $\boldsymbol{\varphi}_{Li}$. As the matrices are not symmetric, the eigenvalues are real or come in pairs (λ_j, λ_j^*). If $\boldsymbol{\varphi}_j$ is a (right or left) eigenvector associated to λ_j, then $\boldsymbol{\varphi}_j^*$ is a (right or left) eigenvector associated to λ_j^*. Ref. [9] is suggested for a thorough review of this kind of problem.

The specific topology of the system matrices in Eq. (2) includes the hypothesis that there is no loss effect at the coupling between the structural and acoustic parts, and that the internal loss can be represented using equivalent viscous models. A detailed description of this vibroacoustical formulation and its damping conditions are given by Ref. [8].

2.2 State-space representation

The non-symmetric character of the vibroacoustical system implies the right and left modes must be described separately. This can be done using the state-space representation of Eq. (1):

$$\mathbf{U}\dot{\mathbf{Q}}(t) - \mathbf{A}\mathbf{Q}(t) = \mathbf{F}(t) \tag{5}$$

where

$$\mathbf{U} = \begin{bmatrix} \mathbf{C} & \mathbf{M} \\ \mathbf{M} & \mathbf{0} \end{bmatrix},\ \mathbf{A} = \begin{bmatrix} \mathbf{-K} & \mathbf{0} \\ \mathbf{0} & \mathbf{M} \end{bmatrix},\ \mathbf{Q}(t) = \begin{Bmatrix} \mathbf{q}(t) \\ \dot{\mathbf{q}}(t) \end{Bmatrix},\ \mathbf{F}(t) = \begin{Bmatrix} \mathbf{f}(t) \\ 0 \end{Bmatrix}. \tag{6}$$

Eigenvalues of Eq. (5) are stored in the spectral matrix $\mathbf{\Lambda} = \begin{bmatrix} \ddots & & \\ & \lambda_j & \\ & & \ddots \end{bmatrix}$. The corresponding eigenvalue problem can then be represented as

$$(\mathbf{U}\lambda_i - \mathbf{A})\boldsymbol{\theta}_{Ri} = \mathbf{0} \tag{7}$$

and

$$\boldsymbol{\theta}_{Li}^T(\mathbf{U}\lambda_i - \mathbf{A}) = \mathbf{0} \tag{8}$$

where $\boldsymbol{\theta}_{Ri}$ and $\boldsymbol{\theta}_{Li}$ are respectively the *i*-th right and left eigenvectors, with the construction as:

$$\boldsymbol{\theta}_{Ri} = \begin{bmatrix} \boldsymbol{\varphi}_{Ri} \\ \boldsymbol{\varphi}_{Ri}\lambda_i \end{bmatrix},\ \boldsymbol{\theta}_{Li} = \begin{bmatrix} \boldsymbol{\varphi}_{Li} \\ \boldsymbol{\varphi}_{Li}\lambda_i \end{bmatrix} \tag{9}$$

where $\boldsymbol{\varphi}_{Ri}$ and $\boldsymbol{\varphi}_{Li}$ are respectively the *i*-th right and left eigenvectors of Eq. (1). $\boldsymbol{\theta}_{Ri}$ and $\boldsymbol{\theta}_{Li}$ can also be constructed in modal matrix form:

$$\boldsymbol{\Theta}_R = \begin{bmatrix} \Phi_R \\ \Phi_R\mathbf{\Lambda} \end{bmatrix},\ \boldsymbol{\Theta}_L = \begin{bmatrix} \Phi_L \\ \Phi_L\mathbf{\Lambda} \end{bmatrix}. \tag{10}$$

Then Eq. (7) and Eq. (8) can be respectively formulated as

$$\mathbf{U}\boldsymbol{\Theta}_R\mathbf{\Lambda} = \mathbf{A}\boldsymbol{\Theta}_R \tag{11}$$

and

$$\mathbf{U}^T\boldsymbol{\Theta}_L\mathbf{\Lambda} = \mathbf{A}^T\boldsymbol{\Theta}_L\ . \tag{12}$$

Let $\boldsymbol{\xi} = \begin{bmatrix} \ddots & & \\ & \xi_j & \\ & & \ddots \end{bmatrix}$ denotes a diagonal matrix with 2*n* arbitrary diagonal elements, the orthogonality between different modes can be represented as

$$\boldsymbol{\Theta}_L^T\mathbf{U}\boldsymbol{\Theta}_R = \boldsymbol{\xi} \text{ or } \boldsymbol{\Theta}_L^T\mathbf{A}\boldsymbol{\Theta}_R = \boldsymbol{\xi}\mathbf{\Lambda}\ . \tag{13}$$

The modal decomposition of the permanent harmonic response at frequency ω is

$$\mathbf{Q}(t) = \boldsymbol{\Theta}_R(\boldsymbol{\xi}(\mathrm{i}\omega\mathbf{E}_{2n} - \mathbf{\Lambda}))^{-1}\boldsymbol{\Theta}_L^T\mathbf{F}(\omega)e^{\mathrm{i}\omega t} \tag{14}$$

where $\mathbf{E}_{2n}$ is the 2*n*-by-2*n* identity matrix and $\mathbf{F}(\omega)$ is the complex amplitude of the harmonic excitation. This relationship can also be written using the *n* dofs notion in the frequency domain as

$$\mathbf{Q}(\omega) = \Phi_R\mathbf{\Xi}\Phi_L^T\mathbf{f}(\omega) \tag{15}$$

where

$$\mathbf{\Xi} = \begin{bmatrix} \backslash & & \\ & \dfrac{1}{\xi_i(\mathrm{i}\omega - \lambda_i)} & \\ & & \backslash \end{bmatrix}. \tag{16}$$

It is important to note in the following context, the arbitrary diagonal matrix $\boldsymbol{\xi}$ in Eq. (13) is assumed to be normalized as $\boldsymbol{\xi} = \mathbf{E}_{2n}$. Similarly in Eq. (16), $\xi_i = 1, \forall i = 1, \cdots, n$. This normalization condition is significant in the following inverse procedure to reconstruct the system matrices.

As for a general non-symmetric problem, the right and left eigenvectors are different and have no certain relationship with each other. While in the case of vibroacoustical application, due to the special topology of the problem shown in Eq. (2), there is a direct link between the right and left complex modes [10] :

$$\text{If } \Phi_R = \begin{Bmatrix} \mathbf{X} \\ \mathbf{P} \end{Bmatrix}, \text{ then } \Phi_L = \begin{Bmatrix} \mathbf{X} \\ -\mathbf{P}\boldsymbol{\Lambda}^{-2} \end{Bmatrix} \tag{17}$$

where **X** corresponds to the structural dofs of the right eigenvector, and **P** is related to the acoustic dofs. Note that, this relationship is valid under the situation with only viscous damping and without structural-acoustic cross damping. This hypothesis is fundamental for the vibroacoustical problem considered in this paper and it is also important for the least-square complex frequency-domain (LSCF) identification method introduced in the following section.

3 Enforcement of the properness condition

The inverse procedure to reconstruct the system matrices from the complex modes can be derived starting from the orthogonality relationship in Eq. (13). When $\boldsymbol{\xi}$ is normalized to $\mathbf{E}_{2n}$ (the normalization condition), it is easy to calculate the inverse of **U** and **A** as:

$$\begin{aligned} \mathbf{U}^{-1} &= \boldsymbol{\Theta}_R \boldsymbol{\Theta}_L^T \\ \mathbf{A}^{-1} &= \boldsymbol{\Theta}_R \boldsymbol{\Lambda} \boldsymbol{\Theta}_L^T \end{aligned} . \tag{18}$$

Recalling Eqs. (6) and (10), the above equations can be rewritten as

$$\begin{aligned} \begin{bmatrix} \mathbf{C} & \mathbf{M} \\ \mathbf{M} & 0 \end{bmatrix}^{-1} &= \begin{bmatrix} \Phi_R \Phi_L^T & \Phi_R \boldsymbol{\Lambda} \Phi_L^T \\ \Phi_R \boldsymbol{\Lambda} \Phi_L^T & \Phi_R \boldsymbol{\Lambda}^2 \Phi_L^T \end{bmatrix} \\ \begin{bmatrix} -\mathbf{K} & 0 \\ 0 & \mathbf{M} \end{bmatrix}^{-1} &= \begin{bmatrix} \Phi_R \boldsymbol{\Lambda}^{-1} \Phi_L^T & \Phi_R \Phi_L^T \\ \Phi_R \boldsymbol{\Lambda} \Phi_L^T & \Phi_R \boldsymbol{\Lambda} \Phi_L^T \end{bmatrix} \end{aligned} . \tag{19}$$

Then the system matrices are extracted as

$$\begin{aligned} \mathbf{M} &= \left[\Phi_R \boldsymbol{\Lambda} \Phi_L^T \right]^{-1} \\ \mathbf{K} &= -\left[\Phi_R \boldsymbol{\Lambda}^{-1} \Phi_L^T \right]^{-1} \\ \mathbf{C} &= -\left[\mathbf{M} \Phi_R \boldsymbol{\Lambda}^2 \Phi_L^T \mathbf{M} \right] \end{aligned} . \tag{20}$$

The above inverse procedure is valid only if the so-called properness condition is satisfied, which can be easily yielded from Eq. (19) as

$$\Phi_R \Phi_L^T = 0 . \tag{21}$$

Note that the above properness condition is universal for the entire non-symmetric problem. For the particular vibroacoustical case, the properness condition can be rewritten using only the right complex eigenvector as

$$\begin{bmatrix} \mathbf{X}\mathbf{X}^T & -\mathbf{X}\boldsymbol{\Lambda}^{-2}\mathbf{P}^T \\ \mathbf{P}\mathbf{X}^T & -\mathbf{P}\boldsymbol{\Lambda}^{-2}\mathbf{P}^T \end{bmatrix} = 0 . \tag{22}$$

Identified from the experimental measurements, the complex eigenvectors are unavoidably polluted by the random noise, which comes from both of the measurements and the identification process. As a result, the identified complex modes generally do not verify the properness condition, which means an enforcement procedure is required before the modes can be utilized in the inverse procedure to reconstruct the system matrices. This enforcement procedure is essentially an optimization problem:

Finding the approximate $\tilde{\mathbf{X}}$ and $\tilde{\mathbf{P}}$, minimizing $f_1 = \| \tilde{\mathbf{X}} - \mathbf{X} \|$ and $f_2 = \| \tilde{\mathbf{P}} - \mathbf{P} \|$, with the constraints as

$$\begin{cases} g_1 = \tilde{\mathbf{X}}\tilde{\mathbf{X}}^T = 0; \\ g_2 = \tilde{\mathbf{X}}\tilde{\mathbf{P}}^T = 0; \\ g_3 = \tilde{\mathbf{X}}\mathbf{\Lambda}^{-2}\tilde{\mathbf{P}}^T = 0; \\ g_4 = \tilde{\mathbf{P}}\mathbf{\Lambda}^{-2}\tilde{\mathbf{P}}^T = 0. \end{cases} \tag{23}$$

As long as the structural and acoustic parts of the right eigenvector are optimized, the left eigenvector is constructed following Eq. (17).

To solve this optimization problem is not easy because of the eigenvalue matrix $\mathbf{\Lambda}$ which makes it impossible to find explicitly the expression of multipliers versus the unknown vectors. This paper utilizes the so-called "over-properness" enforcement approach, which is described in Ref. [8]. It is possible to obtain quick results that can be used in practical engineering. The general procedure is briefly recalled here.

Firstly, a hybrid matrix combining both the right and left eigenvectors is constructed as

$$\mathbf{\Psi} = \begin{bmatrix} \mathbf{X} \\ \mathbf{P} \\ -\mathbf{P}\mathbf{\Lambda}^{-2} \end{bmatrix}. \tag{24}$$

Considering the properness condition $\mathbf{\Psi}\mathbf{\Psi}^T = 0$, one can get the constraints as

$$\mathbf{\Psi}\mathbf{\Psi}^T = \begin{bmatrix} \mathbf{X}\mathbf{X}^T & \mathbf{X}\mathbf{P}^T & -\mathbf{X}\mathbf{\Lambda}^{-2}\mathbf{P}^T \\ \mathbf{P}\mathbf{X}^T & \mathbf{P}\mathbf{P}^T & -\mathbf{P}\mathbf{\Lambda}^{-2}\mathbf{P}^T \\ -\mathbf{P}\mathbf{\Lambda}^{-2}\mathbf{X}^T & -\mathbf{P}\mathbf{\Lambda}^{-2}\mathbf{P}^T & \mathbf{P}\mathbf{\Lambda}^{-4}\mathbf{P}^T \end{bmatrix} = 0. \tag{25}$$

The usage of $\mathbf{\Psi}$ simplifies the problem from a vibroacoustical situation to the typically symmetric structural situation. The methodology proposed in Ref. [11] can be easily employed here by solving a Riccati equation. This equation is derived from the simplified optimization problem:

$$\text{Find } \tilde{\mathbf{\Psi}} \text{ minimizing } \| \tilde{\mathbf{\Psi}} - \mathbf{\Psi} \|, \text{ while } \tilde{\mathbf{\Psi}}\tilde{\mathbf{\Psi}}^T = 0. \tag{26}$$

Note that the obtained $\tilde{\mathbf{\Psi}}$ contains totally six constraints presented in Eq. (25), among which the four required terms of Eq. (23) are included. There are two superfluous constraints which are not theoretically required, and this is the reason why this procedure is called as over-properness enforcement. Nevertheless, as the four required constraints are indeed fulfilled, the procedure gives feasible identification results.

4 Identification and reduction techniques

4.1 Extension of the LSCF identification method

The classical LSCF method has been demonstrated as a reliable technique to identify the complex modes from experimental measurements [12, 13]. While this method is initially developed for symmetric systems, an extension of the LSCF method should be considered for a non-symmetric application. As stated in Ref. [14], the full identification of the right and left eigenvectors requires the excitation being added at every point of sensors, i.e. at every model dofs of interest. However, as a special case of non-symmetric problems, the vibroacoustical system's right and left eigenvectors have a certain relationship as shown in Eq. (17). In this case, only one excitation is needed to perform the full identification.

The first step of the method is to identify the complex poles λ_i from the measured frequency response functions (FRFs), and this can be done in exactly the same way as if the system were symmetric, since the eigenvalues associating with the right and left eigenvectors are equal. Once the poles have been identified, the right and left eigenvectors are calculated based on the so-called *residue matrix*. Construction of the residue matrix is relative to the position of the excitation. Assume the excitation is added on the *k*-th dof of the vibroacoustical system, the residue matrix has the formation as

$$\mathbf{Re}_k = \Phi_R \mathbf{L}_k \tag{27}$$

where Φ_R is the unknown right eigenvector matrix; $\mathbf{L}_k$ is the so-called modal participation matrix, which is diagonal and whose terms are the *k*-th row of the unknown left eigenvector matrix. This indicates each column of $\mathbf{Re}_k$ is proportional to a right eigenvector. Note that according to the excitation is added on the structural or acoustic part of the vibroacoustical system, the proportional coefficients in $\mathbf{Re}_k$ are different, which means the calculation of eigenvectors belongs to different situations.

- **When the excitation is added on the structural part:**

Vector form of Eq. (27) is rewritten as

$$\mathbf{Re}_k = \begin{bmatrix} \cdots & \boldsymbol{\varphi}_{Ri} & \cdots \end{bmatrix} \begin{bmatrix} \ddots & & \\ & x_{ki} & \\ & & \ddots \end{bmatrix} \tag{28}$$

where $\boldsymbol{\varphi}_{Ri}, \forall i = 1, \cdots, n$, is the *i*-th right eigenvector; $x_{ki}, \forall i = 1, \cdots, n,$ is the unknown coefficient. As x_{ki} is simultaneously the element in the *k*-th row of the left eigenvector which belongs to the structural dofs , it is clear to get

$$x_{ki} = \sqrt{\mathbf{Re}_k(k,i)}, \forall i = 1, \cdots, n \tag{29}$$

where $\mathbf{Re}_k(k,i)$ is the element positioned at the *k*-th row and *i*-th column in matrix $\mathbf{Re}_k$. Then the right eigenvector is extracted as

$$\boldsymbol{\varphi}_{Ri} = \frac{\mathbf{Re}_k(:, i)}{x_{ki}}, \forall i = 1, \cdots, n \tag{30}$$

where $\mathbf{Re}_k(:, i)$ is the *i*-th column of $\mathbf{Re}_k$, afterwards the left eigenvector is calculated following Eq. (17).

- **When the excitation is added on the acoustic part:**

In this case, vector form of Eq. (27) should be rewritten in a different formation compared with Eq. (28):

$$\mathbf{Re}_k = \begin{bmatrix} \cdots & \boldsymbol{\varphi}_{Ri} & \cdots \end{bmatrix} \begin{bmatrix} \ddots & & \\ & -p_{ki}\lambda_i^{-2} & \\ & & \ddots \end{bmatrix} \tag{31}$$

where $p_{ki}, \forall i = 1, \cdots, n,$ is the unknown coefficient with the same sense as x_{ki} in Eq. (28). p_{ki} is simultaneously the element in the *k*-th row of the left eigenvector, but herein it belongs to the acoustic part, which can be calculated as

$$p_{ki} = \sqrt{-\mathbf{Re}_k(k,i)\lambda_i^2}, \forall i = 1, \cdots, n . \tag{32}$$

Then the right eigenvector is extracted as

$$\boldsymbol{\varphi}_{Ri} = -\frac{\mathbf{Re}_k(:, i)}{p_{ki}\lambda_i^2}, \forall i = 1, \cdots, n . \tag{33}$$

Similarly, the left eigenvector can be obtained following Eq. (17).

4.2 QR decomposition for model reduction

Model reduction is popular in the fields such as structural dynamics, system and controlling, and numerical mathematics. The objective of model reduction herein is to find an equivalent model with reduced dofs, which continues to exhibit the same system behavior as the full size one.

Ref. [15] describes a methodology based on QR decomposition to optimize the placement of sensors in experimental measurement. Though with different objectives, the activity in Ref. [15] obeys the same logic as which proposed in this work, which is to screen the “key” dofs that can be used to represent the system behavior. Under this sense, the QR decomposition is a suitable technique which can be employed here to achieve this objective.

In order to discriminate the key dofs, the identified full size eigenvector matrix is investigated. The idea is that the most linear independent rows of this matrix construct a reduced matrix which provides a MAC (Modal Assurance Criteria) with minimized off-diagonal terms. In other words, these dofs are capable of representing the maximum number of modes. QR decomposition is proposed here to extract these rows from the original eigenvector matrix Φ:

$$\Phi^T \mathbf{E} = \mathbf{QR} \tag{34}$$

where **Q** is an orthogonal matrix; **R** is an upper triangular matrix; **E** is a column permutation matrix with the purpose of making the diagonal terms of **R** are ranked in descending order. The row vectors with the most significant independence can subsequently be discriminated according to the rearranged column number in matrix **E**.

Two principles are fulfilled by this technique when reducing the dofs: i) The selected dofs are sensitive for the maximum number of modes in the frequency range of interest; ii) For a given mode, responses on two selected dofs are different and independent enough to make each of the modes is distinguishable. This is the reason why the technique is feasible not only for optimizing the placement of sensors before the experiment but also for reducing a large size original model after the experiment. The MAC matrix of the reduced model can be employed to evaluate the effect of this technique by checking if the off-diagonal terms are minimized.

5 Application: A large size simulated case

The overall identification process is illustrated by a large size numerical vibroacoustical case study with the following steps:

1. **The original data**: The start point is the system matrices following the specific vibroacoustical topology. The frequency response functions (FRFs) and the coupled/uncoupled natural frequencies are then calculated according to these matrices. The original FRFs and frequencies are served as the reference data in the following procedure.
2. **Identification and reduction**: Based on the original FRFs, the complex modes are identified by the extended LSCF method. The complex eigenvector matrix is reduced from the original size to a much smaller size using the QR decomposition technique. In order to simulate the uncertainty in experimental measurements, the uniform random noise (with the maximum as 1% of the original data) has been added on the eigenvectors and eigenvalues.
3. **The direct data**: The reduced and noised complex modes are then employed in the inverse procedure to reconstruct the system matrices. These matrices are termed as “direct” because they are obtained from the original modes but without optimization. The direct FRFs and frequencies are calculated according to the direct matrices with the purpose for comparison with the original and optimized ones.
4. **The proper data**: The over-properness enforcement procedure is proposed to optimize the reduced complex modes before they can be utilized in the inverse procedure. The optimized system matrices

are termed as “proper” data. And similarly, the proper FRFs and frequencies are calculated according to the proper matrices.

5.1 Identification and reduction of the original data

The proposed vibroacoustical system contains 130 structural dofs and 123 acoustic dofs. The original system matrices with the size of 253-by-253 are pre-defined following the specific vibroacoustical topology. As long as the original FRFs are calculated, an identification procedure based on the extended LSCF method is performed, as shown in Fig. 1. This identification procedure is performed on MODAN, which is an integrated structural dynamic identification software developed by Femto-ST.

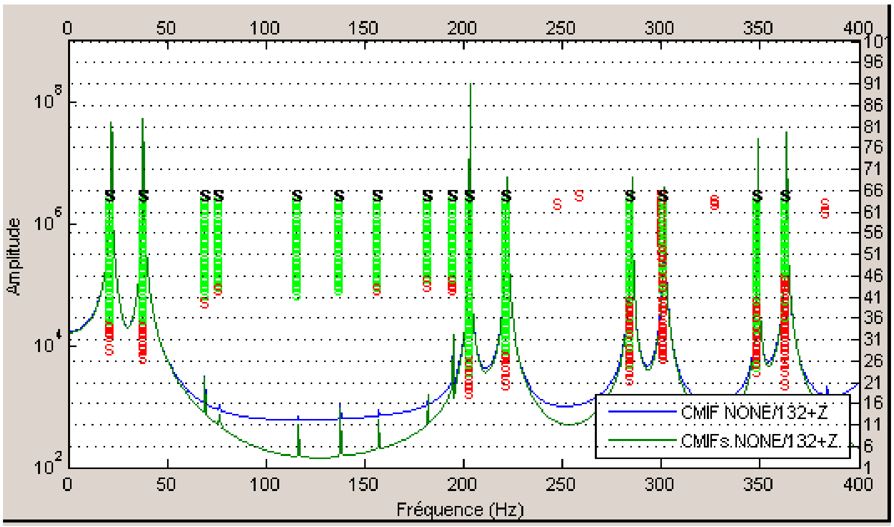

Figure 1: The identification procedure in MODAN

Mode No.	Natural frequencies		
	coupled	structural	Acoustic
1	21.79	***29.54***	28.38
2	***38.16***	***69.79***	202.47
3	***69.35***	***77.10***	221.66
4	***76.64***	***116.76***	283.94
5	***116.42***	***137.90***	301.49
6	***137.65***	***157.35***	348.49
7	***157.07***	***182.42***	363.16
8	***182.20***	***194.96***	
9	***194.65***		
10	202.98		
11	222.03		
12	284.93		
13	301.70		
14	348.77		
15	363.49		

Table 1: The original natural frequencies of the coupled and uncoupled system

In this case, the frequency range of interest is 0-400Hz where totally 15 modes are identified. As long as the eigenvector matrices are identified, the QR decomposition technique can be utilized to reduce their size from 253 to 15. While before performing the reduction, it is necessary to make sure that each of the identified frequencies comes from structural part or acoustic part of the coupled system. As the QR decomposition is applied separately on the structural and acoustic parts, a correct understanding of this distribution on the coupled frequency list is important for determining how many structural/acoustic dofs should be reserved in the reduced model. In practical application, finite element analysis results of the uncoupled part can be used to estimate this first knowledge. While in this case as the original system matrices are available, the exact coupled and uncoupled frequencies are listed in Table 1.

As shown in Table 1, in these 15 modes there are 8 structural modes and 7 acoustic modes, indicating 8 structural dofs and 7 acoustic dofs should be reserved in the reduced model. As mentioned above, the MAC matrix can be utilized to evaluate the effects of reduction. Fig. 2 is the MAC matrices of the reduced and original models, showing the degree of independence among rows in the eigenvector matrices. Both of these two MAC matrices in Fig. 2 are corresponding to the acoustic part of the system, while the difference is that MAC in Fig. 2(a) is for the eigenvector matrix reduced by QR decomposition (termed as MAC_QR); MAC in Fig. 2(b) is for a eigenvector matrix whose 7 rows are randomly selected from the original 130 rows of the acoustic eigenvector matrix (termed as MAC_Random).

The diagonal terms of these two MAC matrices are naturally equal to one, while the off-diagonal terms of them are obviously different. The off-diagonal terms of MAC_QR are basically minimized to zero indicating a high degree of independence of the row vectors of the reduced eigenvector matrix. Contrary, the off-diagonal terms of MAC_Random have different values from zero to one, which means some rows in the randomly reduced model are dependent with others, and consequently, they are not the dofs suitable enough to be reserved during model reduction.

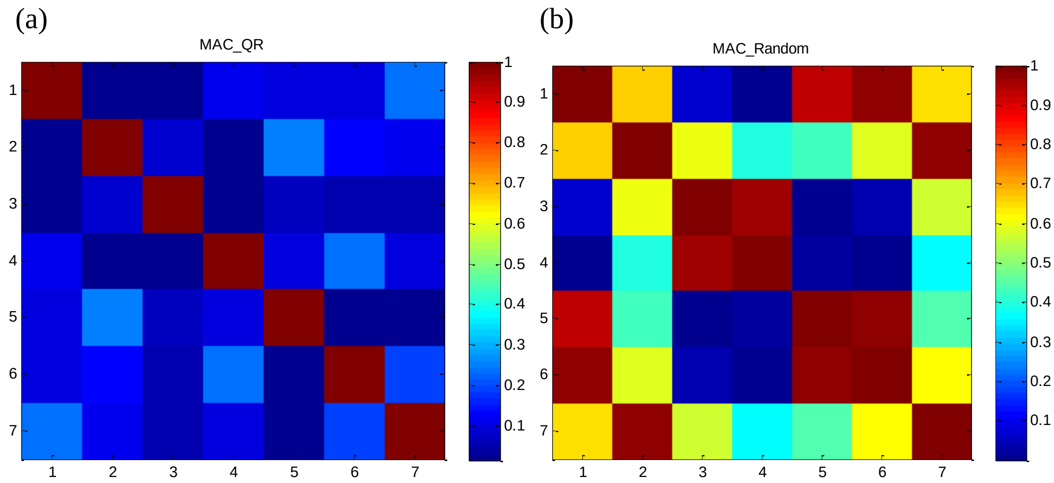

Figure 2: (a) MAC of the QR decomposition reduced model, (b) MAC of the randomly reduced model

5.2 Comparison between the direct and optimized data

The original, direct, and proper FRFs are compared respectively on the structural and acoustic parts of the vibroacoustical system, as shown in Fig. 3.

The direct FRF is calculated based on the matrices which are constructed following Eq. (20). However, the direct eigenvectors do not necessarily fulfill the properness condition. Table 2 shows the Euclidian norm of the properness condition matrix, which is proposed here to denote the degree how the eigenvectors verify the properness condition. It is clear that norm of the proper eigenvector matrix is minimized to a small value, while norm of the direct eigenvector matrix is relatively much larger. This explains the results in Fig. 3 where the direct FRFs are obviously inconsistent with the original FRFs while the proper FRFs fit with the original data well.

	Direct eigenvectors	Proper eigenvectors
Norm of $\Phi_R \Phi_L^T$	273.95	5.13

Table 2: Euclidian norm of the properness condition matrices

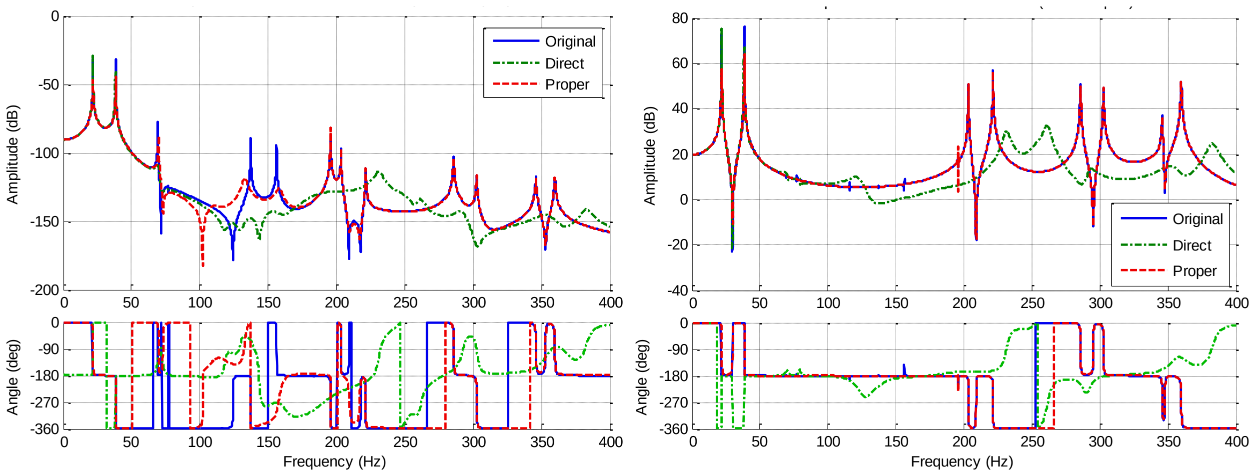

Figure 3: Comparison of FRFs (left: on the 2nd dof - structural part; on the 9th dof - acoustic part)

Results in Fig. 3 show that the identified small size matrices can reproduce the behavior of the original large size system. While it is interesting to check from Fig 3, both of the original and proper FRFs have lost a mode nearby 400 Hz. Explanation for this discrepancy should trace back to the first step of the identification using MODAN. Fig. 1 shows some discrete poles nearby 400 HZ which are not selected. As these modes have been lost in the first step of the process, it is natural that the identified model cannot represent them, even if the model has been optimized. Note that the phenomenon of mode losing during identification is more common in real experimental case when there is more uncontrollable noise in the measurements. Frequencies of the original, direct, and proper models are shown in Table 3. It is clear that the proper frequencies fit the original data with a high precision. However, the direct frequencies display an obvious error compared with the original data.

Mode No.	Natural frequencies		
	Original (Hz)	Direct(Hz)	Proper (Hz)
1	21.79	21.77 (-0.09)	21.74 (-0.23)
2	38.16	38.22 (0.16)	38.49 (0.86)
3	69.35	69.55 (0.29)	67.49 (-2.68)
4	76.64	79.22 (3.37)	71.63 (-6.54)
5	116.42	123.38 (5.98)	121.01 (3.94)
6	137.65	139.37 (1.25)	139.46 (1.32)
7	157.07	153.87 (-2.04)	153.96 (-1.98)
8	182.20	170.66 (-6.33)	180.20 (-1.10)
9	194.65	190.66 (-2.05)	195.74 (0.56)
10	202.98	231.61 (14.10)	203.38 (0.20)
11	222.03	255.44 (15.05)	221.41 (-0.28)
12	284.93	261.52 (-8.22)	285.84 (0.32)
13	301.70	293.64 (-2.67)	302.74 (0.34)
14	348.77	354.57 (1.66)	346.05 (-0.78)
15	363.49	383.66 (5.55)	359.89 (-0.99)
Absolute mean error		4.59%	1.47%

Table 3: The coupled frequencies of the original, direct, and proper models (percent errors in parentheses)

As for this vibroacoustical case, it is also important to compare the uncoupled frequency of the structural and acoustic parts. The natural frequencies of the structural and acoustic parts are respectively detailed in Tables 4 and 5. The comparison results are similar with the coupled ones as the proper uncoupled frequencies have a much higher representation precision compared with the direct identified data. This result shows the identified model can not only reproduce the behavior of the coupled system, but also the behavior of the uncoupled structural/acoustic part.

Mode No.	Natural frequencies		
	Original	Direct	Proper
1	29.54	29.47 (-0.24)	29.70 (0.54)
2	69.79	77.83 (11.52)	67.57 (-3.18)
3	77.10	93.24 (20.93)	72.66 (-5.76)
4	116.76	107.40 (-8.02)	120.19 (2.94)
5	137.90	138.89 (0.72)	139.13 (0.89)
6	157.35	154.18 (-2.01)	154.29 (-1.94)
7	182.42	187.37 (2.71)	180.52 (-1.04)
8	194.96	196.06 (0.56)	195.95 (0.51)
Absolute mean error		5.84%	2.10%

Table 4: The comparison of uncoupled frequencies of the structural part (errors in parentheses)

Mode No.	Natural frequencies		
	Original	Direct	Proper
1	28.38	28.43 (0.18)	28.30 (-0.28)
2	202.47	181.02 (-10.59)	203.34 (0.43)
3	221.66	193.92 (-12.51)	220.68 (-0.44)
4	283.94	279.60 (-1.53)	283.10 (-0.30)
5	301.49	327.78 (8.72)	302.32 (0.28)
6	348.49	338.22 (-2.95)	345.39 (-0.89)
7	363.16	345.68 (-4.81)	359.79 (-0.93)
Absolute mean error		5.90%	0.51%

Table 5: The comparison of uncoupled frequencies of the acoustic part (errors in parentheses)

6 Conclusions and prospects

An integrated approach containing a series of techniques for model identification in vibroacoustics has been proposed. The identified model is not only reduced but also uncoupled, which means not only the full size system but also the uncoupled subsystem can be represented.

The specific topology of vibroacoustical problem is presented beforehand with the purpose for clarifying the validity domain of this approach. As the first step, the classical LSCF identification method is extended to be adaptive to this non-symmetric vibroacoustical problem, and the normalization condition of the identified complex modes is guaranteed. The QR decomposition is subsequently employed to reduce the full size modes to small size equivalent modes. Before using the modes to reconstruct the system matrices, the over-properness enforcement method is proposed to optimize the directly reduced modes, so that the finally obtained model is physical.

A large size simulated case study is proposed with the motivation that the exact behaviors of the coupled and uncoupled systems can be calculated by the original system matrices, which is severed as reference data during the comparison. While feasibility of this approach in practical experimental case should also be evaluated, in this case, the reference data is directly measured from the uncoupled acoustic part (with rigid walls). This experiment setup and evaluation is in operation as the next step of this work.

Acknowledgment

This work was co-financed by the French National Research Agency under grant number ANR-12-JS09-008-COVIA. It has been performed in cooperation with the Labex ACTION program (ANR-11-LABX-0001-01). The authors wish to thank Barbara Roux, Anthony Boillot, Alexis Rogeon and Otmane Zemzem, the students who have contributed to this work, and Bruno Chamont, the low and mid frequency team manager of PSA Groupe, for providing financial support to this project.

References

[1] J.F. Deü, W. Larbi, R. Ohayon, *Vibration and transient response of structural–acoustic interior coupled systems with dissipative interface*, Computer Methods in Applied Mechanics and Engineering, Vol. 197, No. 51–52, (2008), pp. 4894-4905.

[2] N. Hamzaoui, C. Boisson, C. Lesueur, *Vibro-acoustic analysis and identification of defects in rotating mechinery, Part I: Theoretical model*, Journal of Sound and Vibration, Vol. 216, No. 4, (1998), pp. 553-570.

[3] M.C.C. Bampton, J.R.R. Craig, *Coupling of substructures for dynamic analyses*, AIAA Journal, Vol. 6, No. 7, (1968), pp. 1313-1319.

[4] D.D. Klerk, D.J. Rixen, S.N. Voormeeren, *General Framework for Dynamic Substructuring: History, Review and Classification of Techniques*, AIAA Journal, Vol. 46, No. 5, (2008), pp. 1169-1181.

[5] S.R. Ibrahim, *Existence and Normalization of Complex Modes for Post Experimental Use in Modal Analysis*, in: J.M.M. Silva, N.M.M. Maia, editor, *Modal Analysis and Testing, Springer Netherlands, Dordrecht, 1999*, Springer (1999), pp. 441-452.

[6] P. Lancaster, U. Prells, *Inverse problems for damped vibrating systems*, Journal of Sound and Vibration, Vol. 283, No. 3–5, (2005), pp. 891-914.

[7] M. Ouisse, E. Foltête, *On the properness condition for modal analysis of non-symmetric second-order systems*, Mechanical Systems and Signal Processing, Vol. 25, No. 2, (2011), pp. 601-620.

[8] M. Ouisse, E. Foltête, *Model correlation and identification of experimental reduced models in vibroacoustical modal analysis*, Journal of Sound and Vibration, Vol. 342, No. (2015), pp. 200-217.

[9] F. Tisseur, K. Meerbergen, *The quadratic eigenvalue problem*, SIAM Review, Vol. 43, No. 2, (2001), pp. 235-286.

[10] K. Wyckaert, F. Augusztinovicz, P. Sas, *Vibro-acoustical modal analysis: Reciprocity, model symmetry, and model validity*, The Journal of the Acoustical Society of America, Vol. 100, No. 5, (1996), pp. 3172-3181.

[11] E. Balmés, *New results on the identification of normal modes from experimental complex modes*, Mechanical Systems and Signal Processing, Vol. 11, No. 2, (1997), pp. 229-243.

[12] H. Van Der Auweraer, P. Guillaume, P. Verboven, S. Vanlanduit, *Application of a fast-stabilizing frequency domain parameter estimation method*, Journal of dynamic systems, measurement, and control, Vol. 123, No. 4, (2001), pp. 651-658.

[13] B. Peeters, H. Van der Auweraer, P. Guillaume, J. Leuridan, *The PolyMAX frequency-domain method: a new standard for modal parameter estimation?*, Shock and Vibration, Vol. 11, No. 3-4, (2004), pp. 395-409.

[14] I. Bucher, D. Ewins, *Modal analysis and testing of rotating structures*, Philosophical Transactions of the Royal Society of London A: Mathematical, Physical and Engineering Sciences, Vol. 359, No. 1778, (2001), pp. 61-96.

[15] C. Schedlinski, M. Link, *An approach to optimal pick-up and exciter placement*, in: *Proceedings-SPIE the international society for optical engineering,* SPIE international society for optical (1996),

pp. 376-382.